Interaction between supra-thermal particles and turbulence in magnetic confinement devices

A. Di Siena[1]

with

T. Görler[1], E. Poli[1], R. Bilato[1], A. Banón Navarro[1], A. Biancalani[2], N. Bonanomi[1], A. Zocco[3], H. Doerk, D. Jarema, I. Novikau[1], F. Vannini[1], V. Bobkov[1], E. Fable[1], C. Angioni[1], Ye. Kazakov[4], R. Ochoukov[1], P. Schneider[1], M. Weiland[1], I-G. Farcas[5], N. deOliveira-Lopez[1], M.J. Mantsinen[6,7], F. Jenko[1], T. Hayward-Schneider[1], P. Mantica[8], J. Citrin[9], G. Merlo[5], G. Snoep[9], A. Bottino[1], P. Rodriguez-Fernandez[2], N. Howard[2], J. Wright[2], M. Greenwald[2], JET contributors[11], and the ASDEX Upgrade Team[1]

[1] Max Planck Institute for Plasma Physics, Garching, Germany
[2] Léonard de Vinci Engineering School, Paris, France
[2] Max Planck Institute for Plasma Physics, Greifswald, Germany
[4] LPP-ERM/KMS TEX Partner, Brussels, Belgium
[5] The University of Texas at Austin, Austin, Texas, USA
[6] Barcelona Supercomputing Center, Spain
[7] ICREA, Barcelona, Spain
[8] Istituto per la Scienza e Tecnologia dei Plasmi, CNR, Italy
[9] FOM Institute DIFFER, PO Box 6336, 5600 HH Eindhoven, The Netherlands
[10] MIT Plasma Science and Fusion Center, Cambridge, MA 02139, USA
[11] JET, Culham Science Centre, Abingdon, OX14 3DB, UK

Motivation

- In magnetic confinement devices, turbulence is typically driven by plasma micro-instabilities and represents one of the main cause of confinement degradation → quantity of merit is heat flux $Q = \frac{m}{2}\int v_{E\times B|_x} v^2 F_1 d^3v$

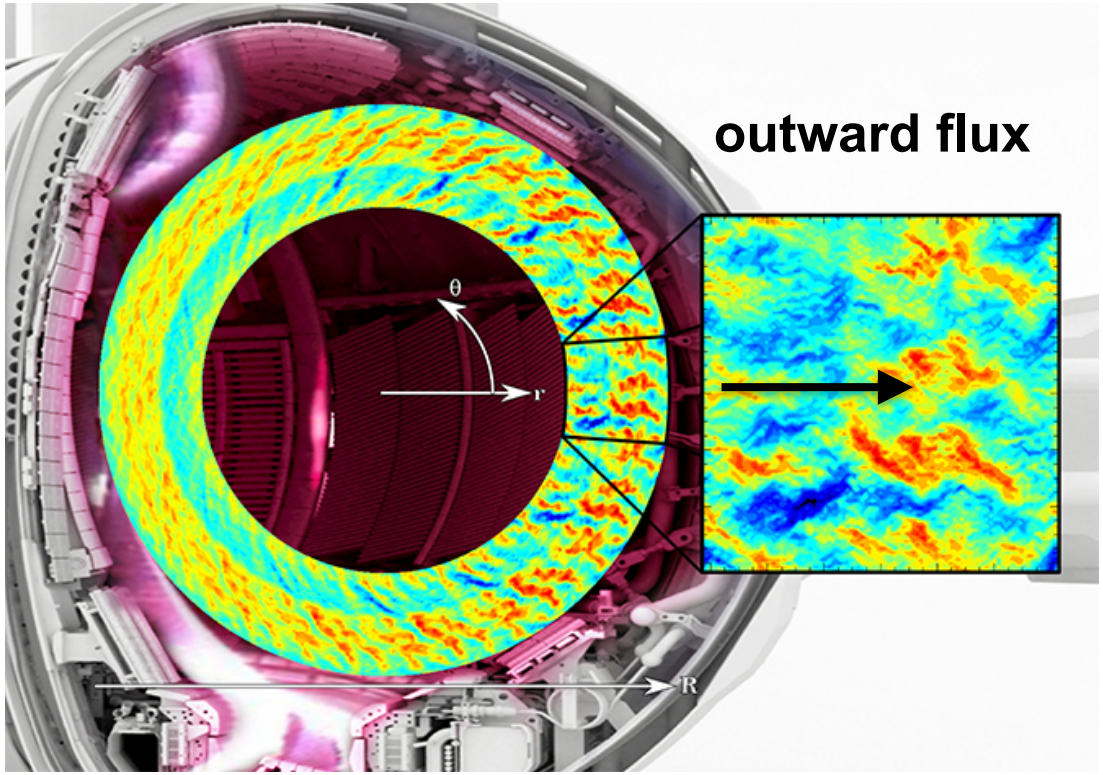

www.pdc.kth.se

Motivation

- 1D transport equation

$$\frac{3}{2}A\frac{\partial p}{\partial t} + \frac{\partial}{\partial x}AQ = AS$$

A: Area flux-surface

S: Sources

$Q = \langle Q \cdot \nabla x \rangle$: Turbulent fluxes

- Q decreases at fixed sources → plasma pressure increase: more fusion output!
- Fast ions have been shown to be an efficient way of suppressing turbulence

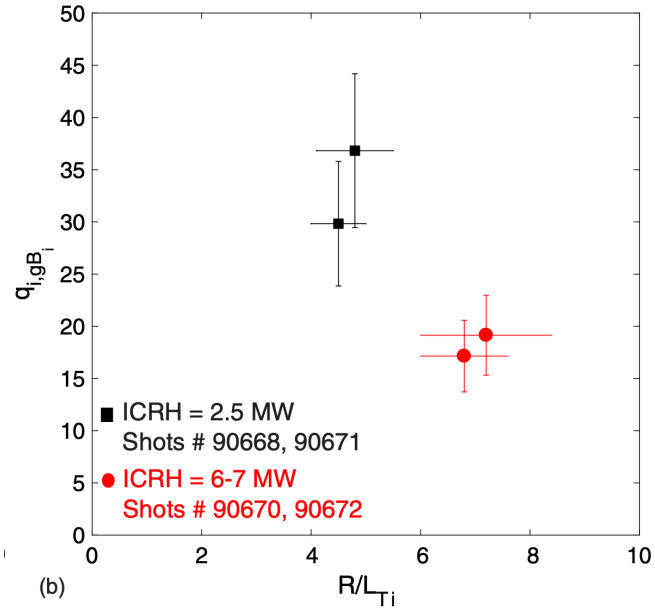

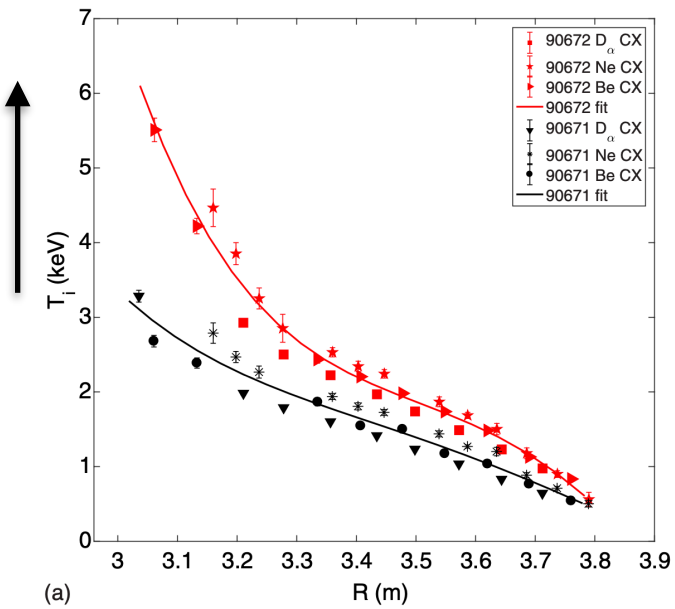

Why and how fast ions suppress turbulence?

Outlook

Nonlinear electromagnetic turbulence suppression by fast particles

- Mode-to-mode coupling between low frequency (ITG) and linearly stable TAE-like modes
- Interaction between EP-driven TAE-like modes and zonal flow
- How good is the flux-tube (local) model in modelling EP effects on turbulence?

Wave-particle resonant interaction between fast ions and ITGs

- Optimised discharge at ASDEX Upgrade: improved confinement!
- Radially global GENE turbulence simulations: anomalous transport barrier
- Possible role of F-ATB on SPARC H-mode scenario with 25 MW of ICRH heating

Conclusions

Outlook

Nonlinear electromagnetic turbulence suppression by fast particles

- Mode-to-mode coupling between low frequency (ITG) and linearly stable TAE-like modes
- Interaction between EP-driven TAE-like modes and zonal flow
- How good is the flux-tube (local) model in modelling EP effects on turbulence?

Wave-particle resonant interaction between fast ions and ITGs

- Optimised discharge at ASDEX Upgrade: improved confinement!
- Radially global GENE turbulence simulations: anomalous transport barrier
- Possible role of F-ATB on SPARC H-mode scenario with 25 MW of ICRH heating

Conclusions

Fast ion stabilisation at JET

- The inclusion of fast ions brings the turbulent fluxes close to experimental power balance.
- Possible coupling to fast ion-driven modes. However, no evidence of a nonlinear coupling.

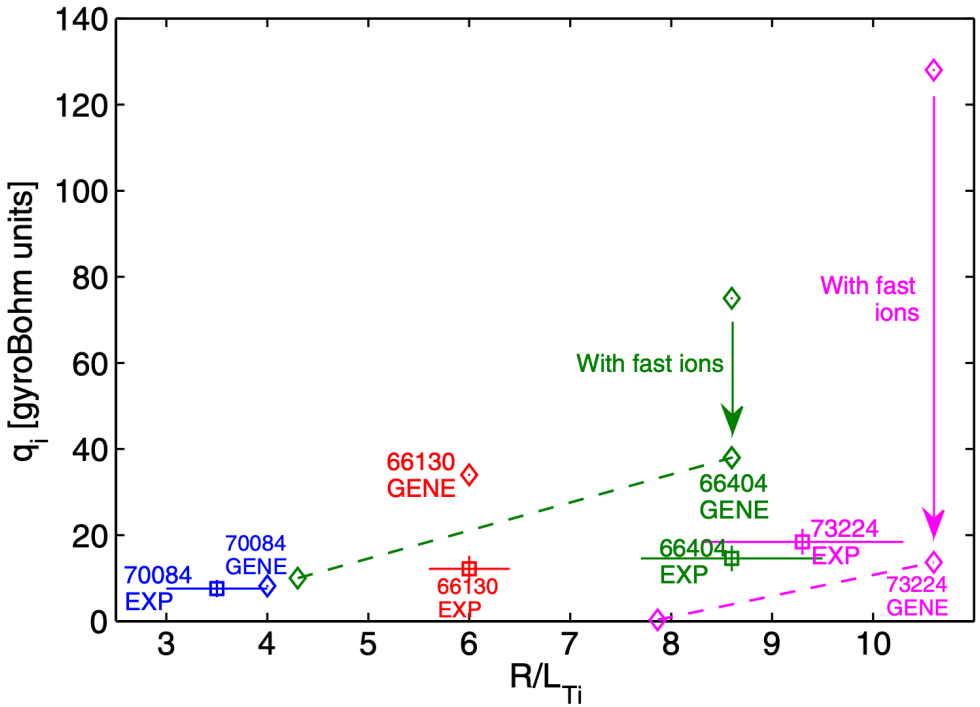

J. Citrin et al. PRL 2013

Fast ion stabilisation at JET

- The inclusion of fast ions brings the turbulent fluxes close to experimental power balance.
- Possible coupling to fast ion-driven modes. However, no evidence of a nonlinear coupling.

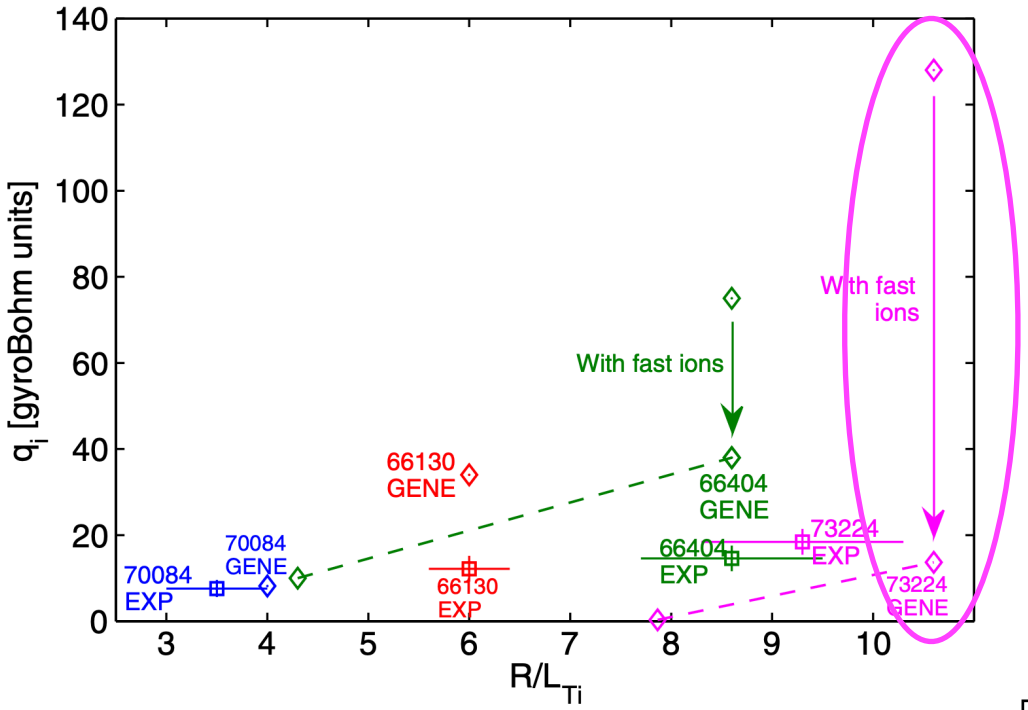

J. Citrin et al. PRL 2013

What is the physics of the nonlinear electromagnetic turbulence suppression by fast ions?

Electromagnetic effects w fast ions

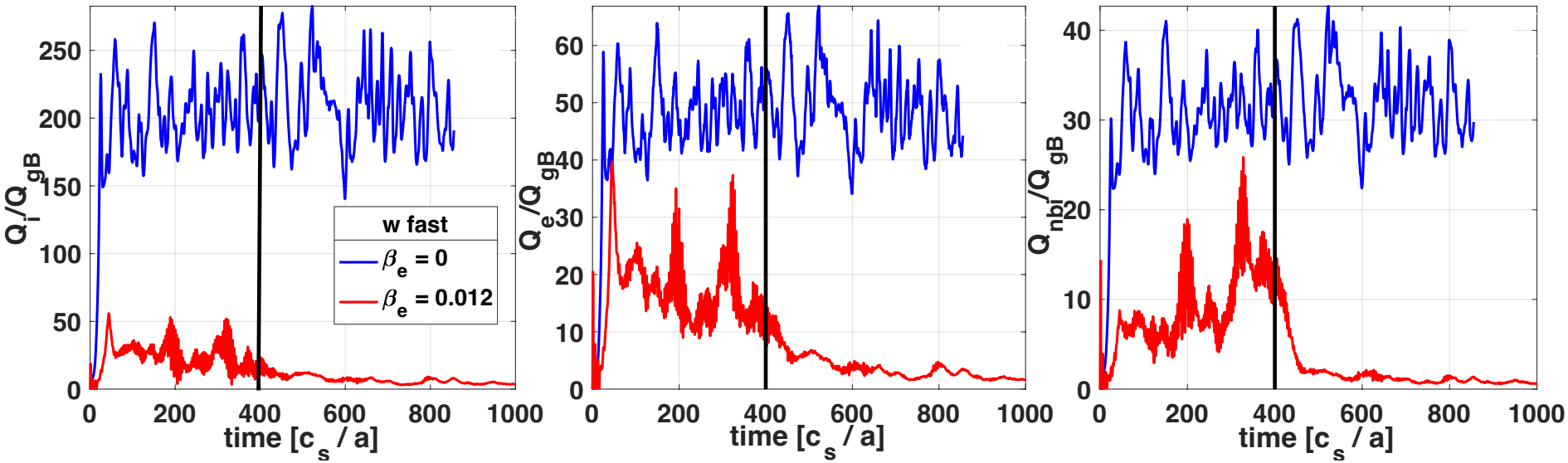

- Substantial heat flux stabilisation in all turbulent channels in the presence of finite β_e-fluctuations (reduced by 95%).
- Two nonlinear phases are identified (remarked by vertical line):
  - Phase 1: high-frequency modulation of the heat flux and slowly decaying transport levels.
  - Phase 2: stationary state at reduced levels.

A. Di Siena et al. NF 2019
A. Di Siena et al. JPP 2021

Physical explanation: ITG-TAE-Zonal flow coupling

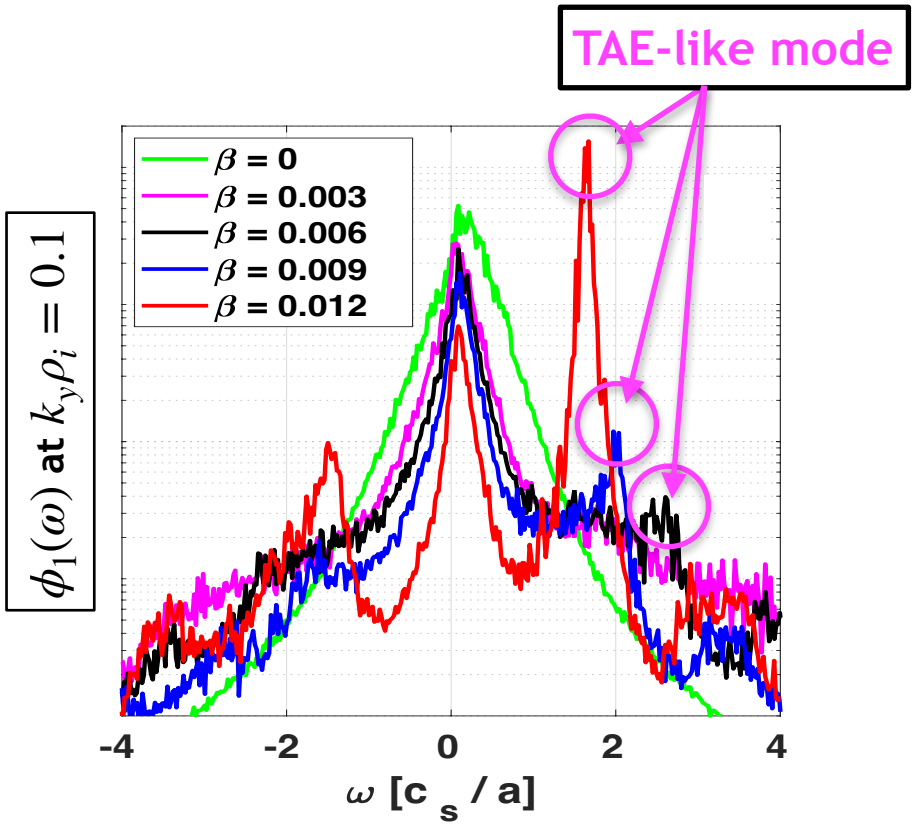

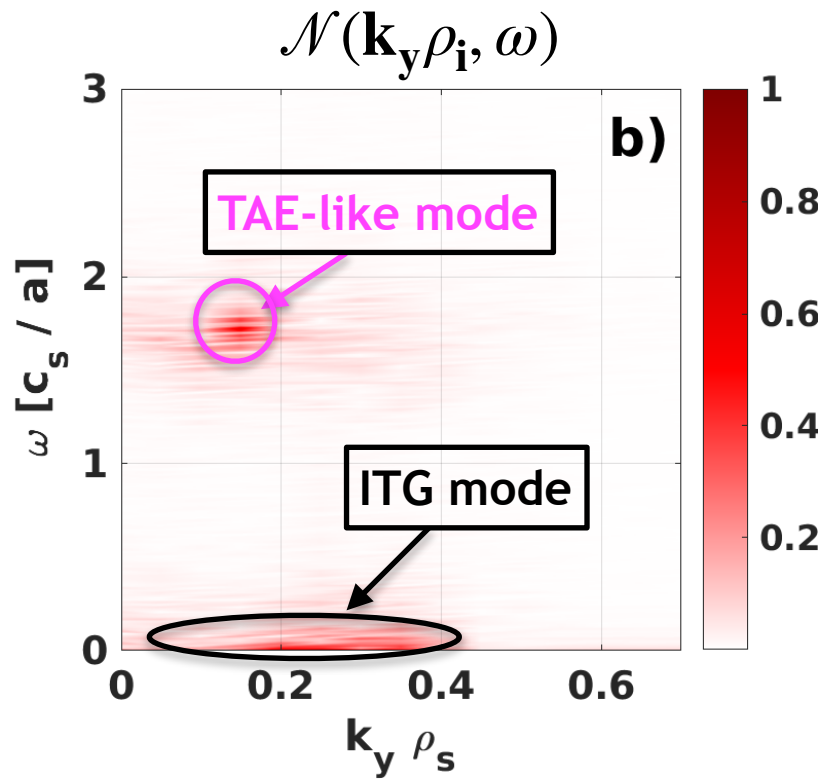

- Progressive destabilisation of **<u>marginally stable</u>** TAE-like mode with β_e only in simulations with fast ions.
- Reduction of ITG peak as TAE-like mode is destabilised.

A. Di Siena et al. NF 2019

Transition to a second stationary state

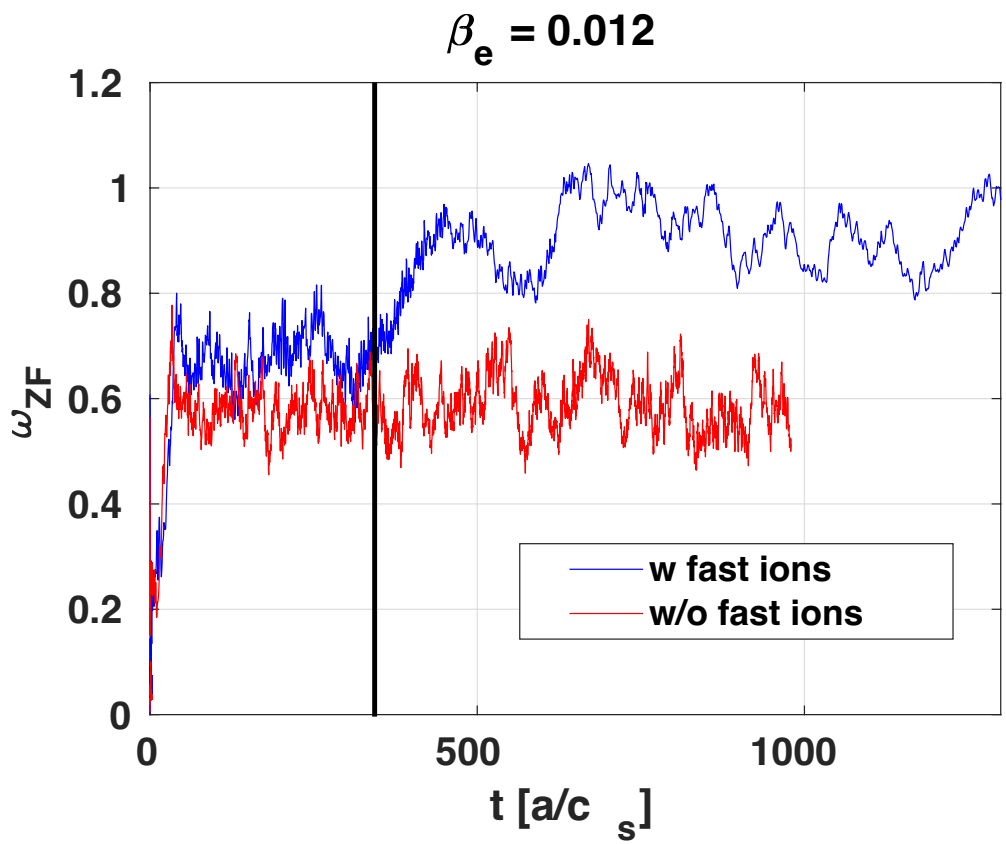

A. Di Siena et al. NF 2019

- Increase in shearing rate levels observed during the transition to the second nonlinear stationary state.
- Detailed free-energy analyses reveal that TAE-like mode starts to interact with zonal flow when reaching sufficiently large amplitudes in Phase I

Physical explanation: ITG-TAE-Zonal flow coupling

Small fast ion drive

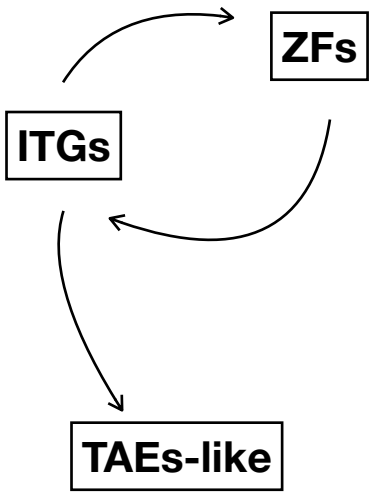

- Fast particles provide linearly stable modes destabilised nonlinearly
- Energy redistribution from thermal to fast ion-driven modes
- Depleting the energy content of the turbulence

Strong fast ion drive

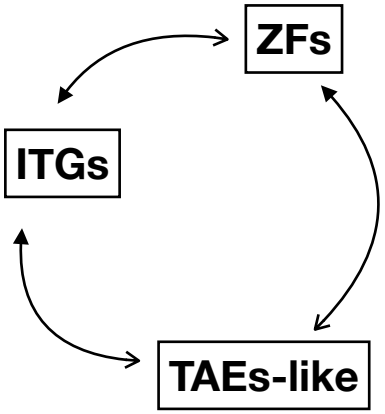

- If the fast ion drive is sufficiently large, fast particle modes interact with zonal flow
- Direct impact of ZF on ITGs, strongly suppressing heat/particle fluxes.

A. Di Siena et al. NF 2019
A. Di Siena et al. JPP 2021

How good is the flux-tube (local) model in modelling EP effects on turbulence?

(Work in progress)

Baseline scenario: L-mode JET #73224

- JET scenario #73224 L-mode plasma, large fast ion content, $B_T = 3.36T, I_p = 1.8MA$, $n_{e,0} = 3.2 \cdot 10^{19} m^{-3}, P_{NBI} = 11MW, P_{ICRH}(^3He) - D = 3MW$

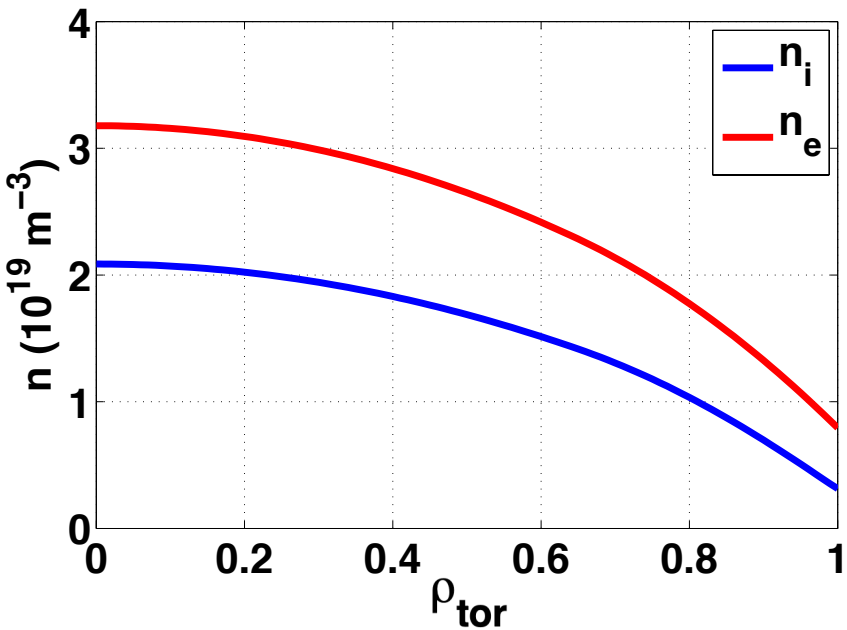

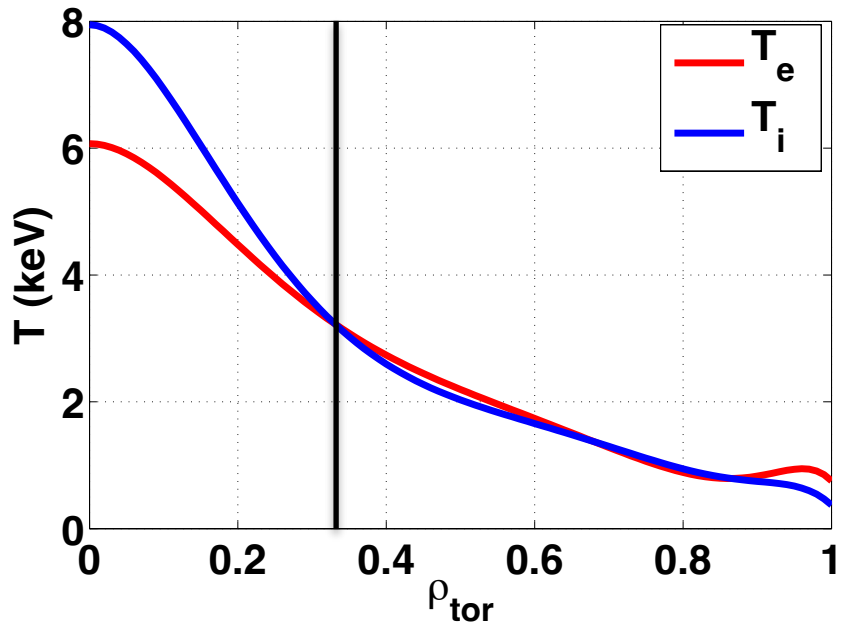

- Fast ions modelled by Maxwellian distribution function

P. Mantica et a. PRL 2009
P. Mantica et al. PRL 2011,
J. Citrin et al. PRL 2013

Global linear simulations

- Radially global GENE simulations are performed covering four different cases: (i) electrostatic limit; (ii) marginally stable FI mode; (iii) weakly unstable FI mode; (iv) strongly unstable FI mode.

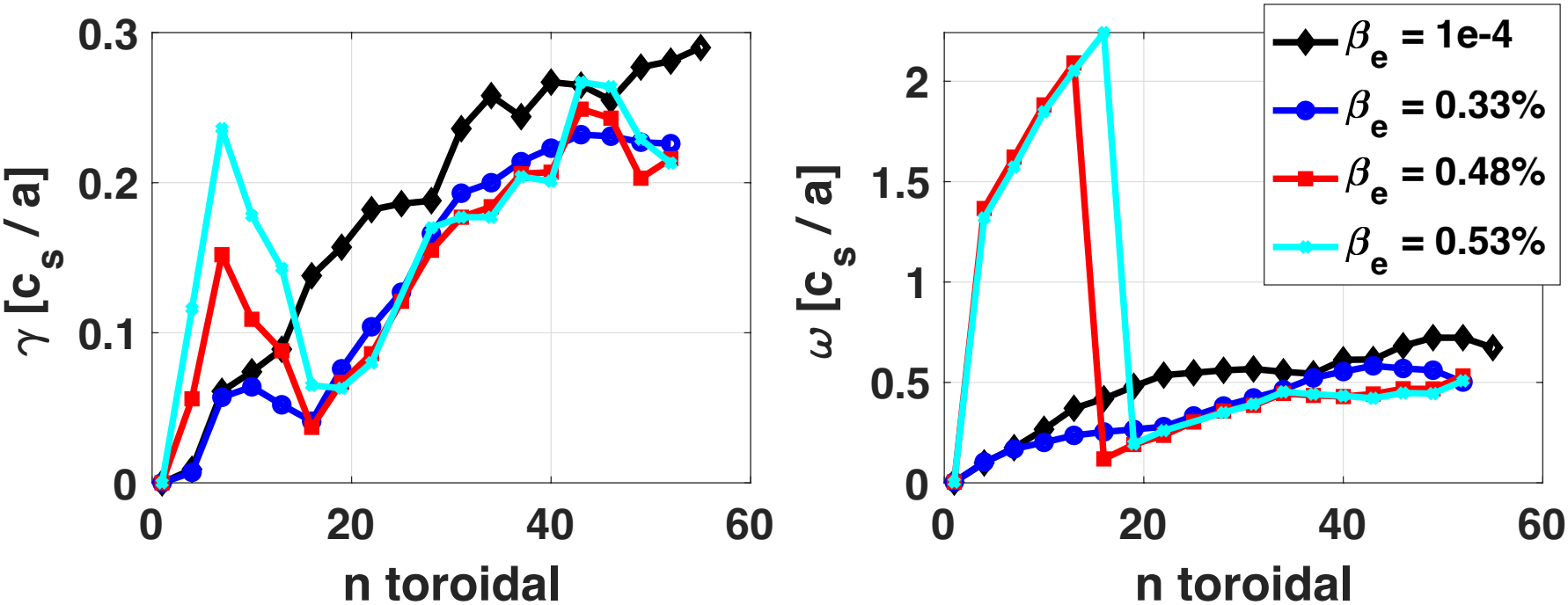

- Fast particle mode grows at high-beta with $\omega[c_s/a] \sim [1.5 - 2]$ located at $\rho_{tor} \sim [0.2 - 0.3]$

Global linear simulations

- Linear flux-tube simulations predict similar range of frequencies and growth rates as the global runs

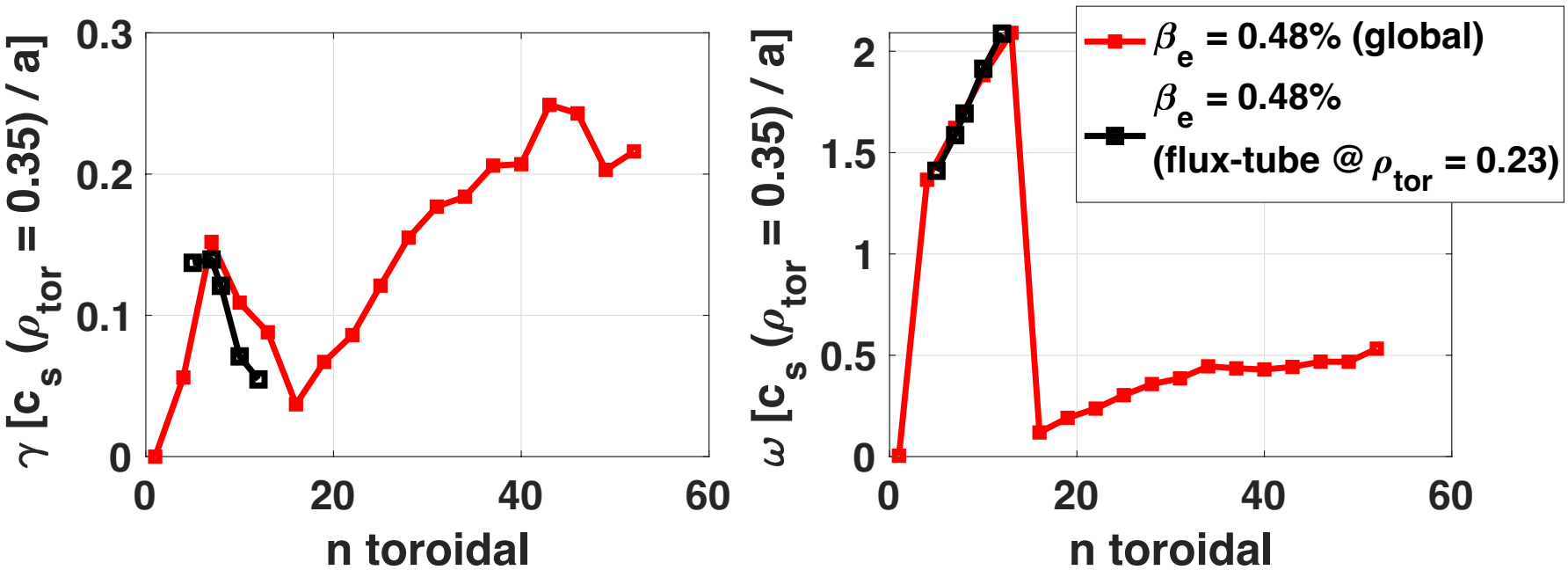

- Fast particle mode grows at high-beta with $\omega[c_s/a] \sim [1.5 - 2]$ located at $\rho_{tor} \sim [0.2 - 0.3]$

Global nonlinear simulations - Turbulent fluxes

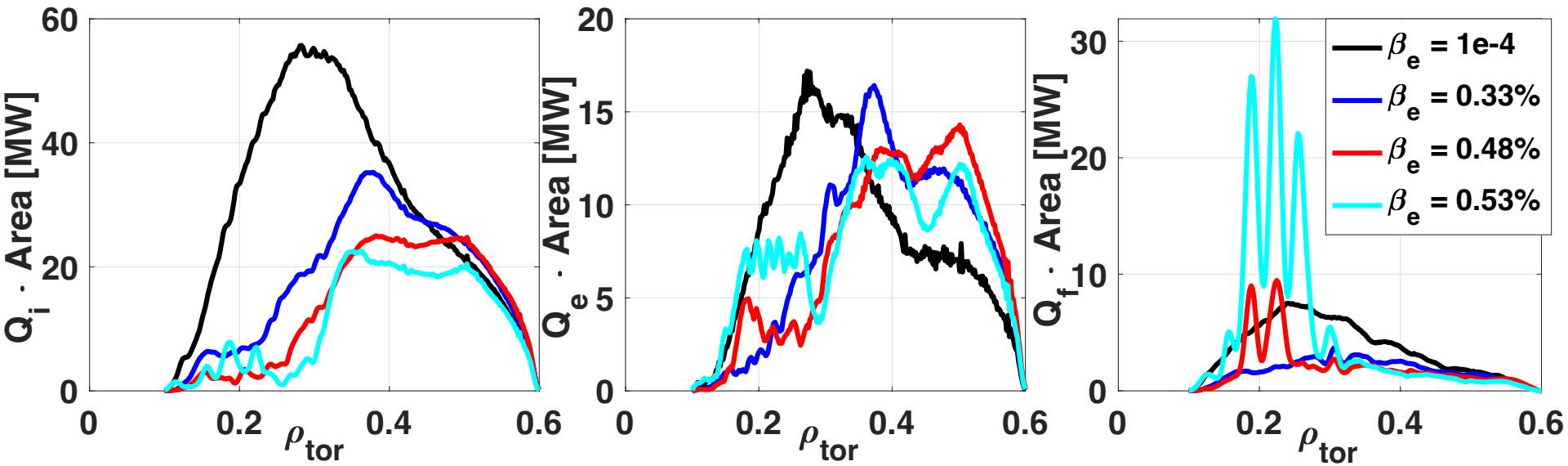

- **Marginally stable FI mode**: turbulent fluxes reduced for all species.
- **Weakly unstable FI mode**: ion heat flux is further reduced; electron and fast ion fluxes increase.
- **Strongly unstable FI mode**: mild increase in ion heat flux; strong increase in electron and fast ion fluxes.

<u>Overall turbulence suppression observed only when FI mode is marginally stable</u>

Comparison global vs flux-tube simulations: $\beta_e = 0$ (electrostatic)

Global vs flux-tube at $\beta_e = 0$ (ES) - Fluxes analyses

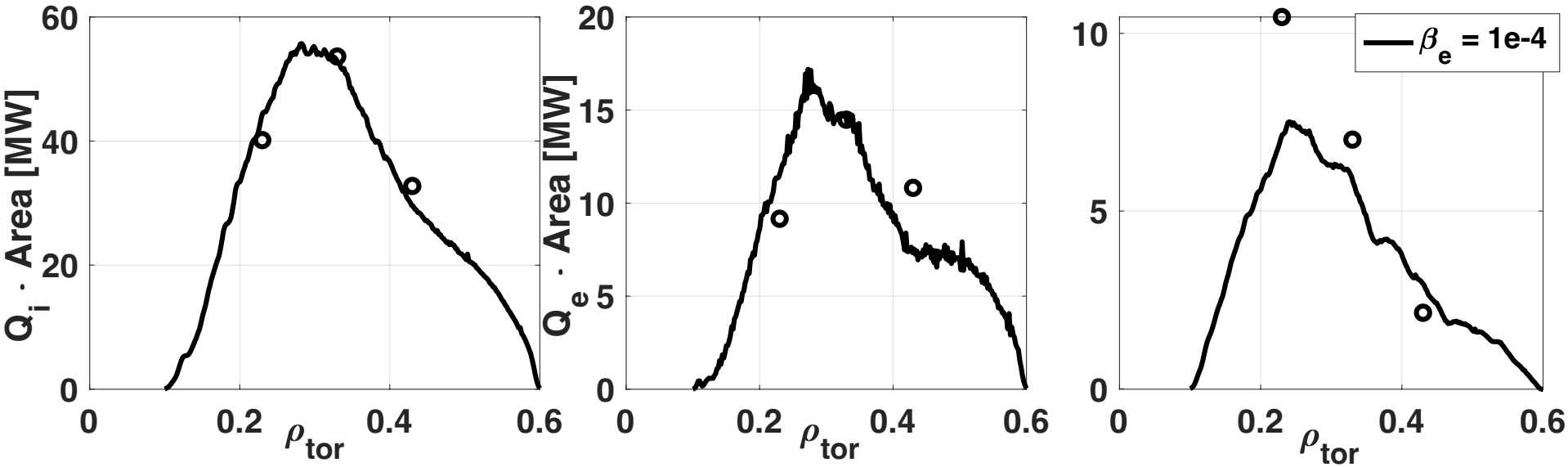

- Excellent agreement with ion and electron heat fluxes.
- Good agreement with fast ion heat flux.

<u>Flux tube simulations can well recover the global turbulent fluxes in the electrostatic limit with fast particles.</u>

Comparison global vs flux-tube simulations: $\beta_e = 0.33\ \%$ (nominal)

Global vs flux-tube at $\beta_e = 0.033$ (nominal - marginally stable EP modes) - Fluxes analyses

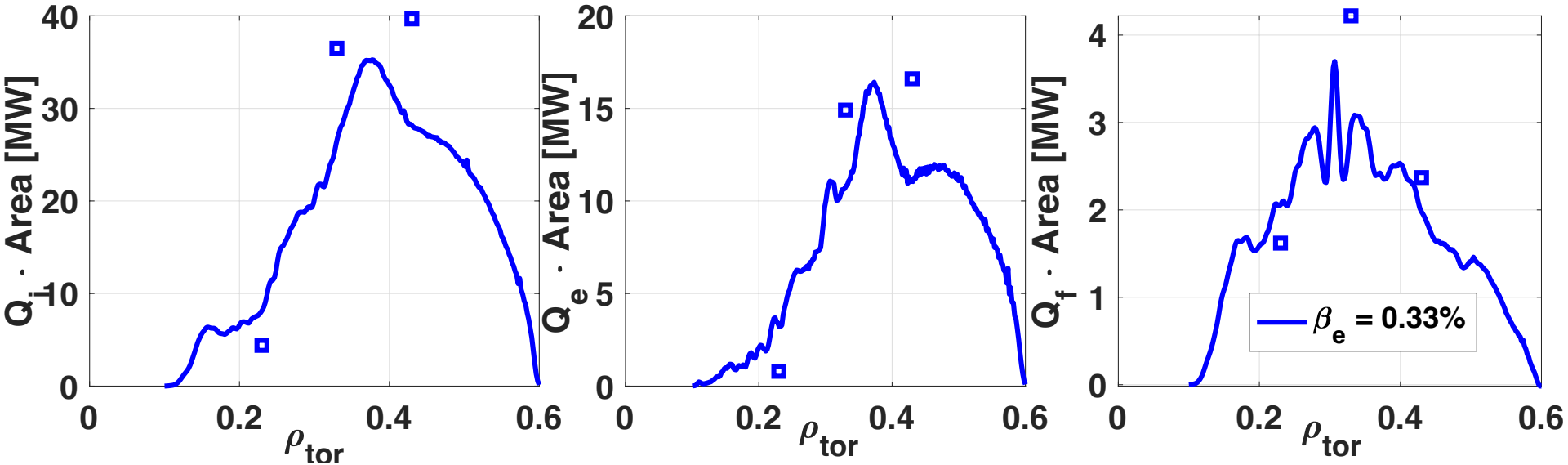

- Good agreement between flux-tube and global fluxes for all different species.

<u>Flux tube simulations can well recover the global turbulent fluxes when the energetic particle modes are marginally unstable and destabilised nonlinearly.</u>

Global vs flux-tube at $\beta_e = 0.033$ (nominal - marginally stable EP modes) - Frequency analyses

- Flux-tube frequency spectra is compared with the one obtained from the global simulation at same location of the flux-tube run
- Flux-tube averaged over k_x, global at $\rho_{tor} = 0.23$ (more noise).

flux-tube

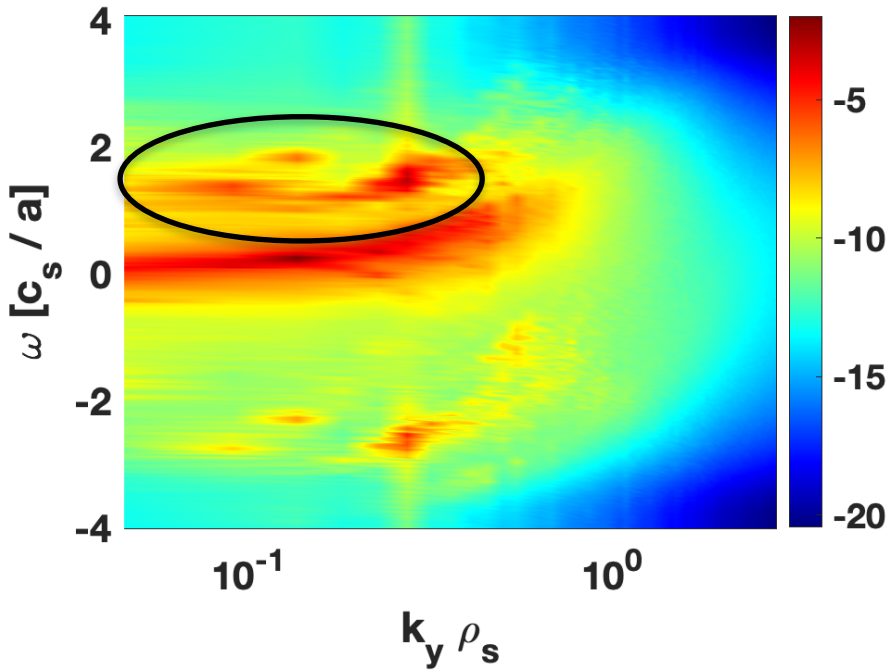

global - $\rho_{tor} = 0.23$

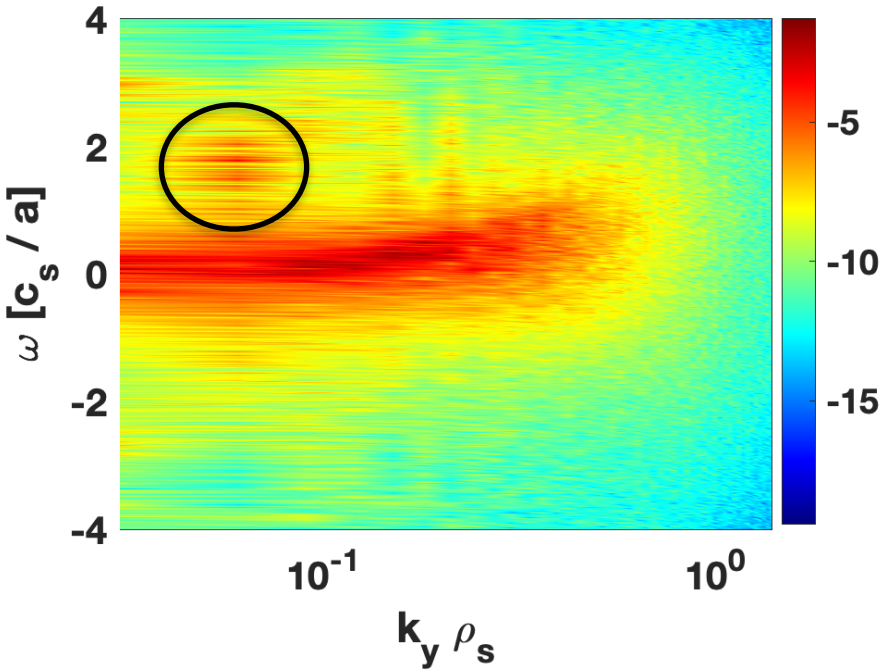

- FI mode present is global simulations

Comparison global vs flux-tube simulations: $\beta_e = 0.48\,\%$ (weakly unstable FI mode)

Global vs flux-tube at $\beta_e = 0.048$ (weakly unstable EP modes) - Fluxes analyses

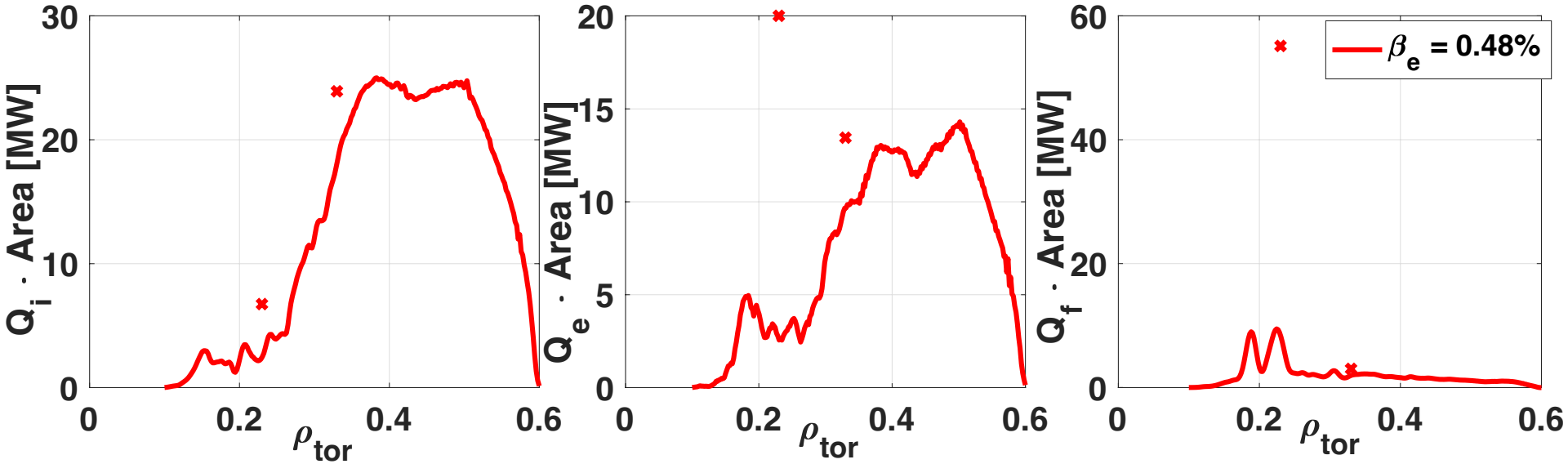

- Good agreement with the thermal ion heat fluxes.
- Flux-tube simulations predict extremely large electron and fast ion heat fluxes, not consistent with the global fluxes.

<u>Flux-tube approximation seems to fail in capturing turbulent fluxes when the fast particle mode is linearly unstable.</u>

Outlook

Nonlinear electromagnetic turbulence suppression by fast particles

- Mode-to-mode coupling between low frequency (ITG) and linearly stable TAE-like modes
- Interaction between EP-driven TAE-like modes and zonal flow
- How good is the flux-tube (local) model in modelling EP effects on turbulence?

Wave-particle resonant interaction between fast ions and ITGs

- Optimised discharge at ASDEX Upgrade: improved confinement!
- Radially global GENE turbulence simulations: anomalous transport barrier
- Possible role of F-ATB on SPARC H-mode scenario with 25 MW of ICRH heating

Conclusions

Are there any other mechanisms from which fast ions can interact with plasma turbulence?

Resonant interaction between ITG and supra-thermal particles

- Unexpected depedence of the linear ITG growth rates with energetic particle temperature in electrostatic simulations!

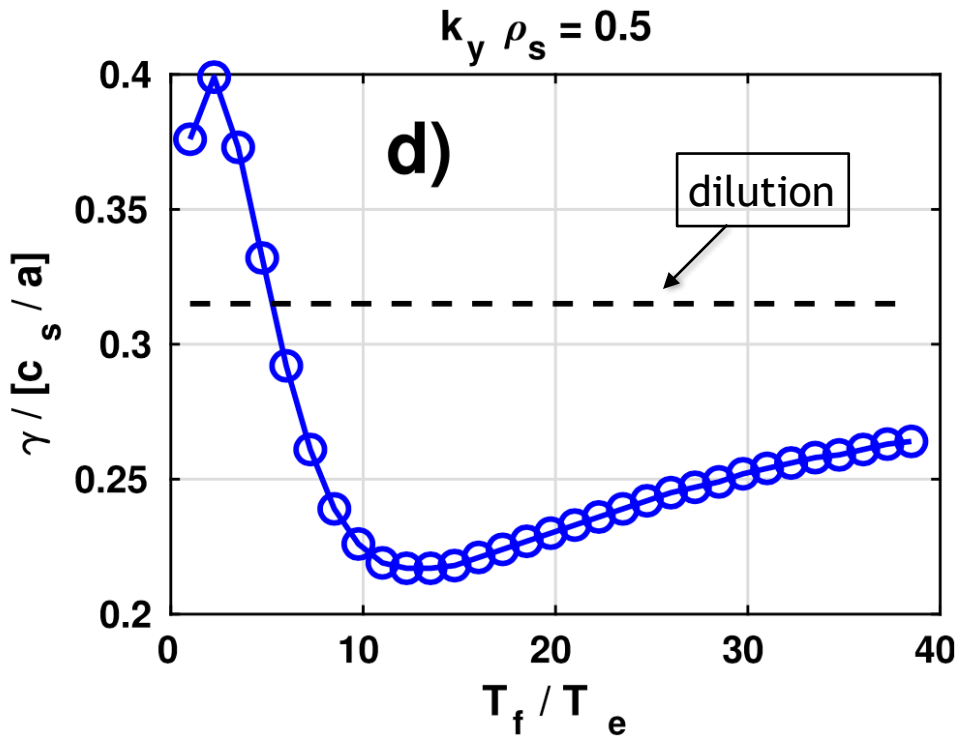

What is the mechanism leading to this strong linear stabilization?

Resonant interaction between ITG and supra-thermal particles

- Supra-thermal particles can interact with ITGs when fast ion magnetic drift frequency $\omega_{d,f}(\propto B_0 \times \nabla B_0)$ is close to the linear ITG frequency ω_k.

A. Di Siena et al. NF 2018
A. Di Siena et al. PoP 2019
A. Di Siena et al. PRL 2020
A. Di Siena et al. PRL 2021

Resonant interaction:

1. energetic particles can resonate with the background instabilities if

$$\omega_k \approx \omega_{d,f}$$

$\omega_{d,f}$ is controlled by T_f

2. effective stabilisation only if

$$\left|\frac{R}{L_{n,f}}\right| \ll \left|\frac{R}{L_{T,f}}\right|$$

Condition typically matched by ICRH fast ions

Resonant interaction between ITG and supra-thermal particles

- Contribution of the fast particle species to the linear growth rate

$$\gamma_f \propto \int n_{0,f} \frac{\gamma_k \left[\frac{R}{L_{n,f}} + \frac{R}{L_{T,f}} \left(v^2 - 1.5 \right) \right]}{\left(\omega_k + \omega_{d,f} \right)^2 + \gamma_k^2} e^{-v^2} v^{3/2} dv$$

A. Di Siena et al. NF 2018
A. Di Siena et al. PoP 2019

$$v^2 = v_{\parallel}^2 + \mu B_0$$

$$L_{n(,T),f} = -\frac{\nabla n(,T)}{n(,T)}$$

Resonant interaction between ITG and supra-thermal particles

- Contribution of the fast particle species to the linear growth rate

A. Di Siena et al. NF 2018
A. Di Siena et al. PoP 2019

$$\gamma_f \propto \int n_{0,f} \frac{\gamma_k \left[\frac{R}{L_{n,f}} + \frac{R}{L_{T,f}} \left(v^2 - 1.5 \right) \right]}{\left(\omega_k + \omega_{d,f} \right)^2 + \gamma_k^2} e^{-v^2} v^{3/2} dv$$

Drift frequency of fast particles

ITG frequency

$$v^2 = v_{\parallel}^2 + \mu B_0$$

$$L_{n(,T),f} = -\frac{\nabla n(,T)}{n(,T)}$$

- wave-fast ions resonance → $\omega_k \approx \omega_{d,f}(T_f)$ maximise fast ion effects

Resonant interaction between ITG and supra-thermal particles

- Contribution of the fast particle species to the linear growth rate

$$\gamma_f \propto \int n_{0,f} \frac{\gamma_k \left[\frac{R}{L_{n,f}} + \frac{R}{L_{T,f}} \left(v^2 - 1.5 \right) \right]}{\left(\omega_k + \omega_{d,f} \right)^2 + \gamma_k^2} e^{-v^2} v^{3/2} dv$$

$\mathscr{K}$

$$v^2 = v_{\parallel}^2 + \mu B_0$$

$$L_{n(,T),f} = -\frac{\nabla n(,T)}{n(,T)}$$

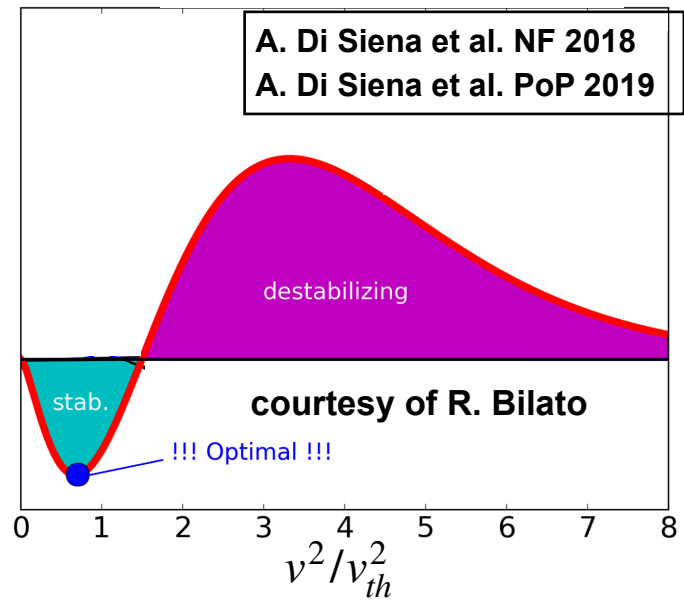

- wave-fast ions resonance $\rightarrow \omega_k \approx \omega_{d,f}(T_f)$ maximise fast ion effects

- Background drive term $\rightarrow$ set direction of energy exchange with micro-instabilities - stabilising only if $R/L_{T,f} \gg R/L_{n,f}$

Resonant interaction between ITG and supra-thermal particles

- Contribution of the fast particle species to the linear growth rate

$$\gamma_f \propto \int n_{0,f} \frac{\gamma_k \left[\frac{R}{L_{n,f}} + \frac{R}{L_{T,f}} \left(v^2 - 1.5 \right) \right]}{\left(\omega_k + \omega_{d,f} \right)^2 + \gamma_k^2} e^{-v^2} v^{3/2} dv$$

$\mathscr{K}$

$$v^2 = v_{\parallel}^2 + \mu B_0$$

$$L_{n(,T),f} = -\frac{\nabla n(,T)}{n(,T)}$$

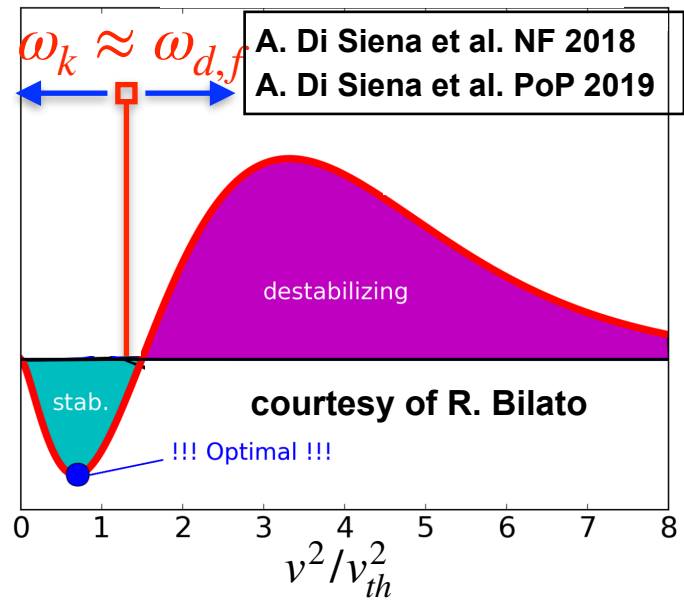

- wave-fast ions resonance $\rightarrow \omega_k \approx \omega_{d,f}(T_f)$ maximise fast ion effects
- Background drive term $\rightarrow$ set direction of energy exchange with micro-instabilities - stabilising only if $R/L_{T,f} \gg R/L_{n,f}$
- Depending on the phase-space localisation of the resonance, this effect might be destabilising as well

Resonant interaction: impact on linear ITGs

- $T_f/T_e < 6$ leads to a linear ITG destabilisation $\rightarrow \omega_k = \omega_{d,f}$ (positive drive region)
- Optimal stabilisation for ^{3}He at $T_f/T_e \sim 12 \rightarrow \omega_k = \omega_{d,f}$ (negative drive region)

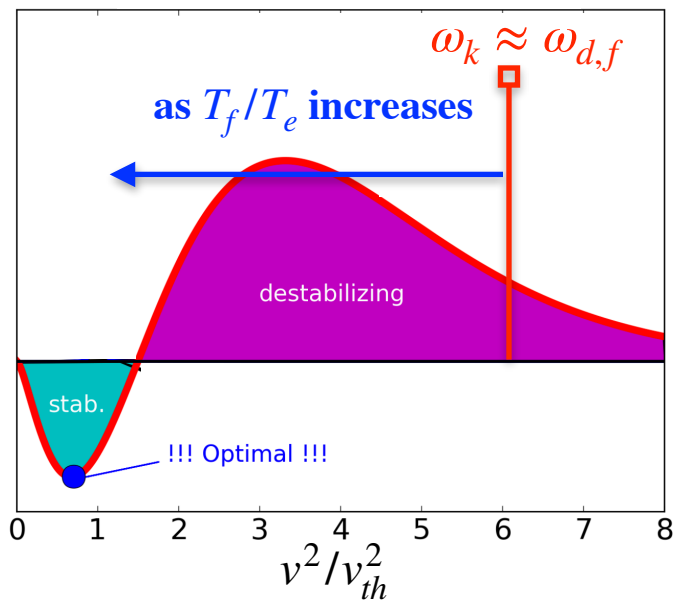

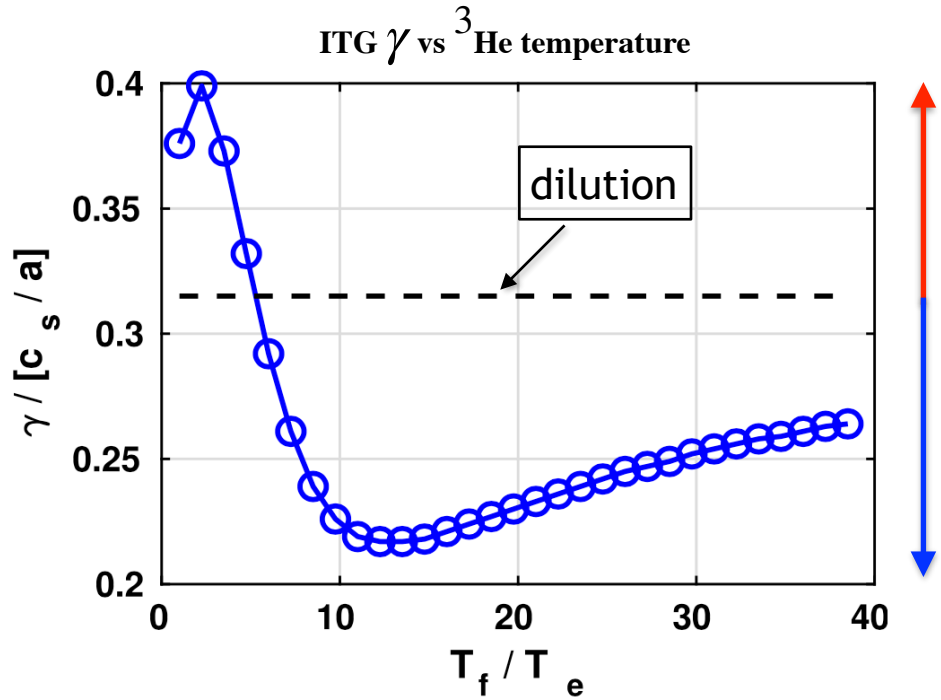

- Depending on the wave-number selected the "sweet-spot" in T_f/T_e for maximum stabilisation changes.

Resonant interaction: nonlinear physics

- $T_f/T_e < 6$ leads to a linear ITG destabilisation $\rightarrow \omega_k = \omega_{d,f}$ (positive drive region)
- Optimal stabilisation for ^{3}He at $T_f/T_e \sim 12 \rightarrow \omega_k = \omega_{d,f}$ (negative drive region)

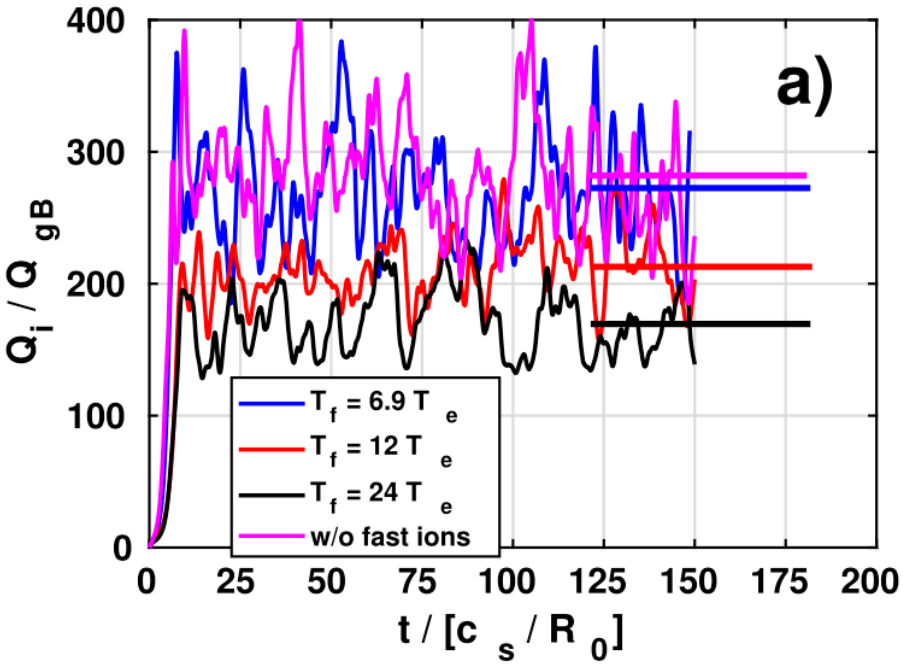

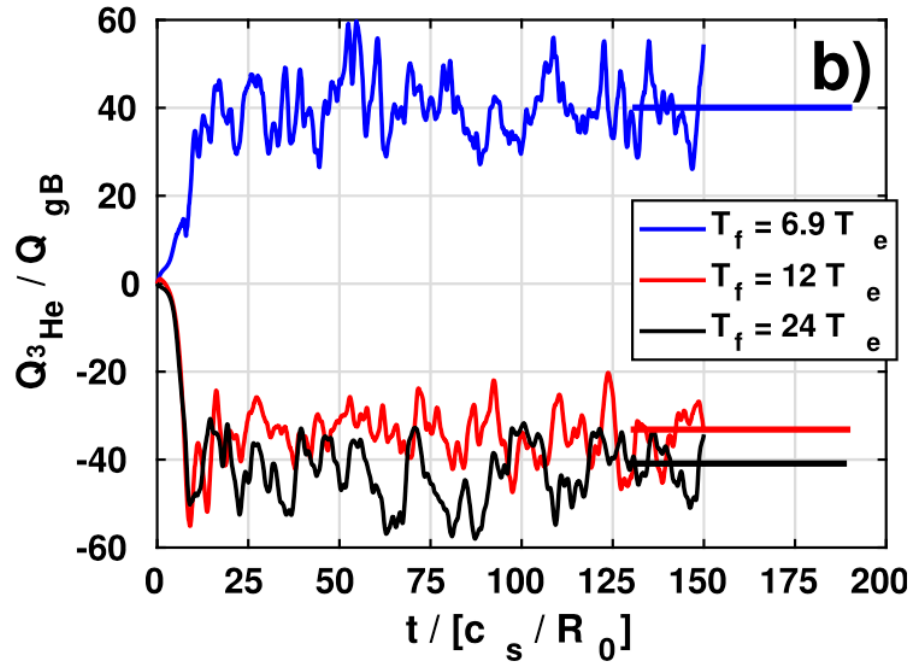

- Depending on the wave-number selected the "sweet-spot" in T_f/T_e for maximum stabilisation changes.

A. Di Siena et al. PoP 2019

How does the wave-particle dynamics change in optimised stellarator devices?

Wave-particle interaction in optimised stellarators

- Strong ITG stabilisation could be achieved also in optimised stellarator devices.
- Tokamaks and stellarators fundamentally different for this resonant interaction → fast ions experience different drift frequencies at each stellarator field-line

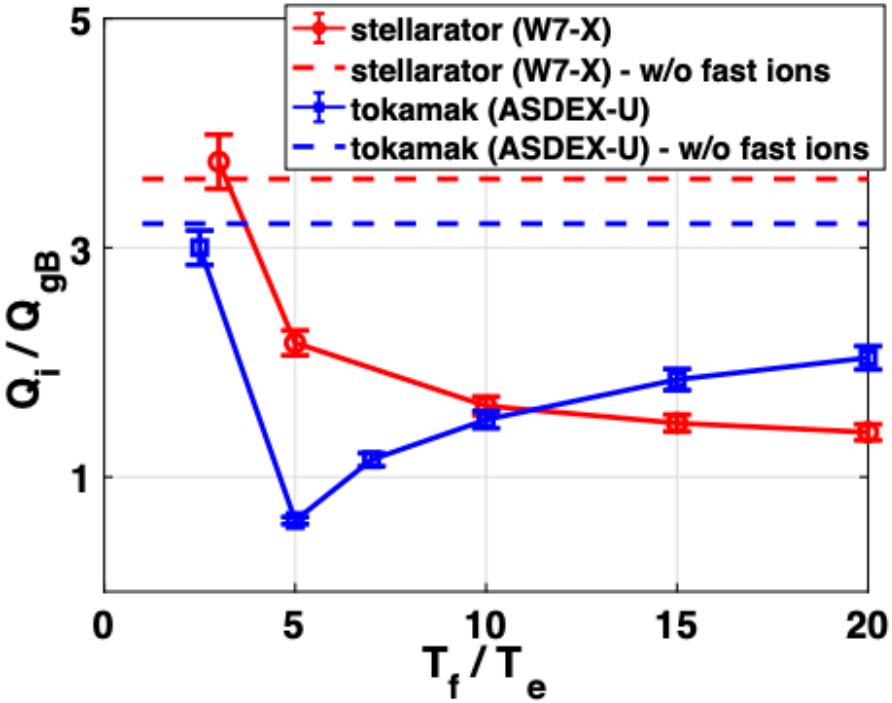

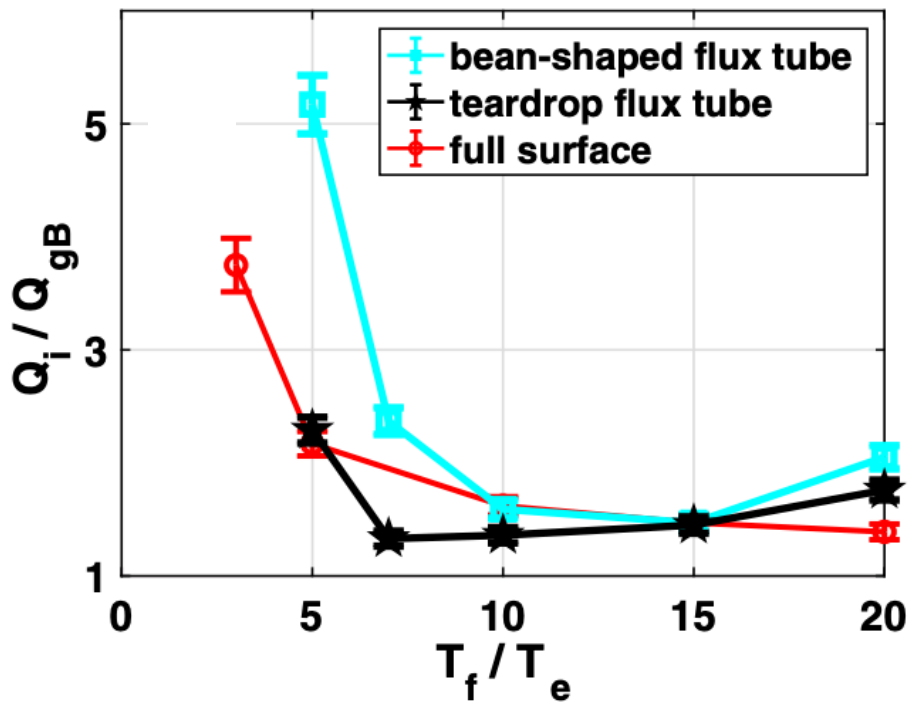

A. Di Siena et al. PRL 2020

Could we exploit this wave-particle resonant interaction to design an optimised discharge?

Internal transport barrier triggered by energetic particle resonant effects

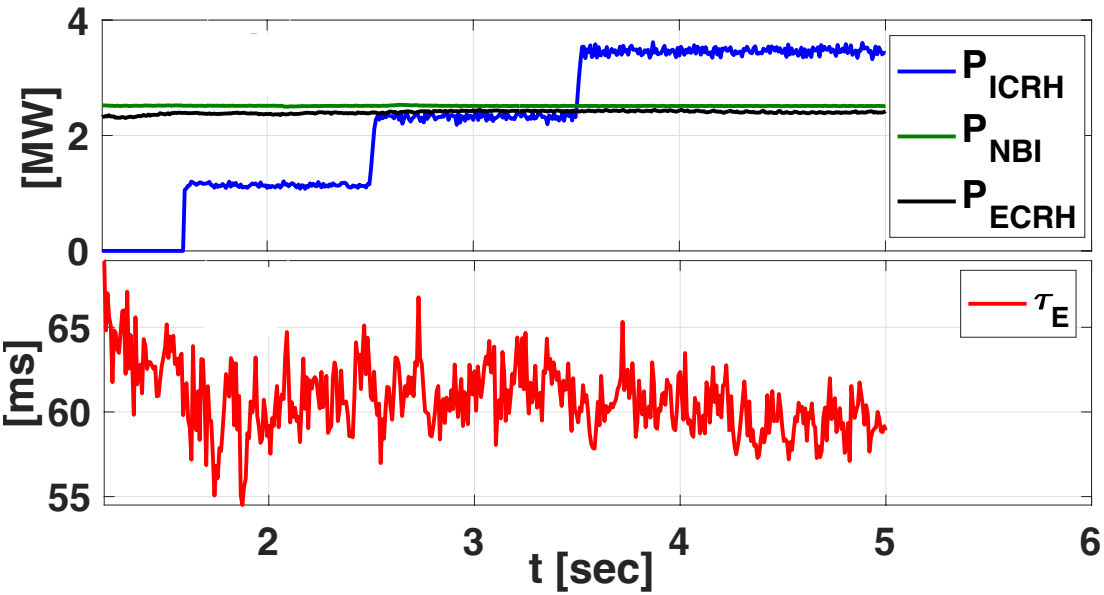

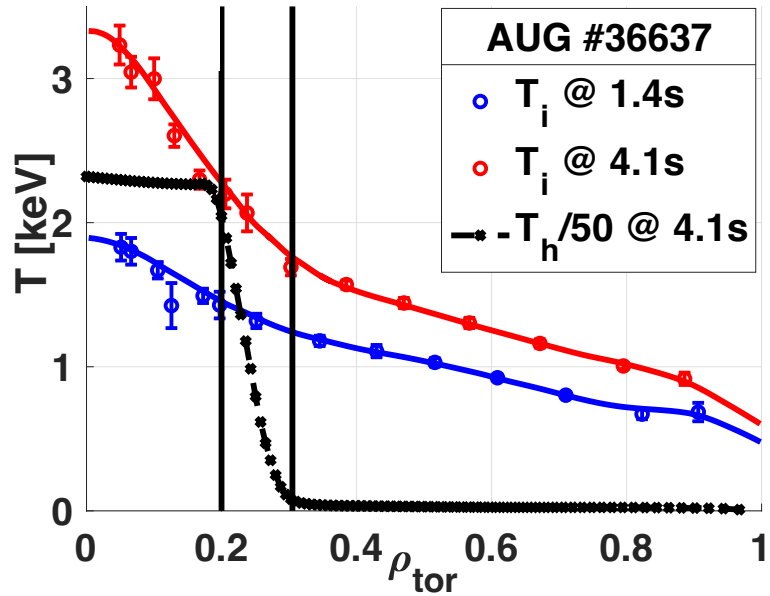

- No degradation of energy confinement time observed by increasing external ICRF power.
- Significant steepening of main ion temperature profile in the region of larger fast ion logarithmic temperature profile

A. Di Siena et al. PRL 2021

Internal transport barrier triggered by energetic particle resonant effects

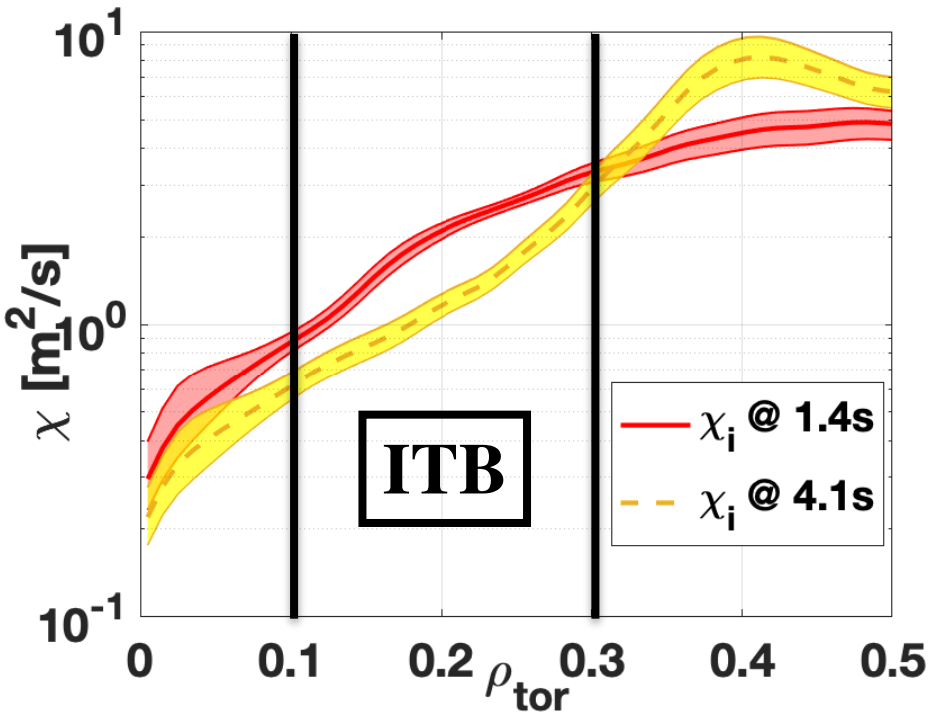

- Ion conductivity at $t = 4.1s$ is reduced by $\sim 50\,\%$ despite the $\sim 40\,\%$ increase of the auxiliary heating.
- Electron conductivity remains at similar levels.

A. Di Siena et al. PRL 2021

Beneficial effect of ICRF observed at AUG

Radial profiles of overall heat fluxes

- Internal transport barrier observed in radially global GENE simulations by looking at the overall (ion + fast ions) ion heat flux

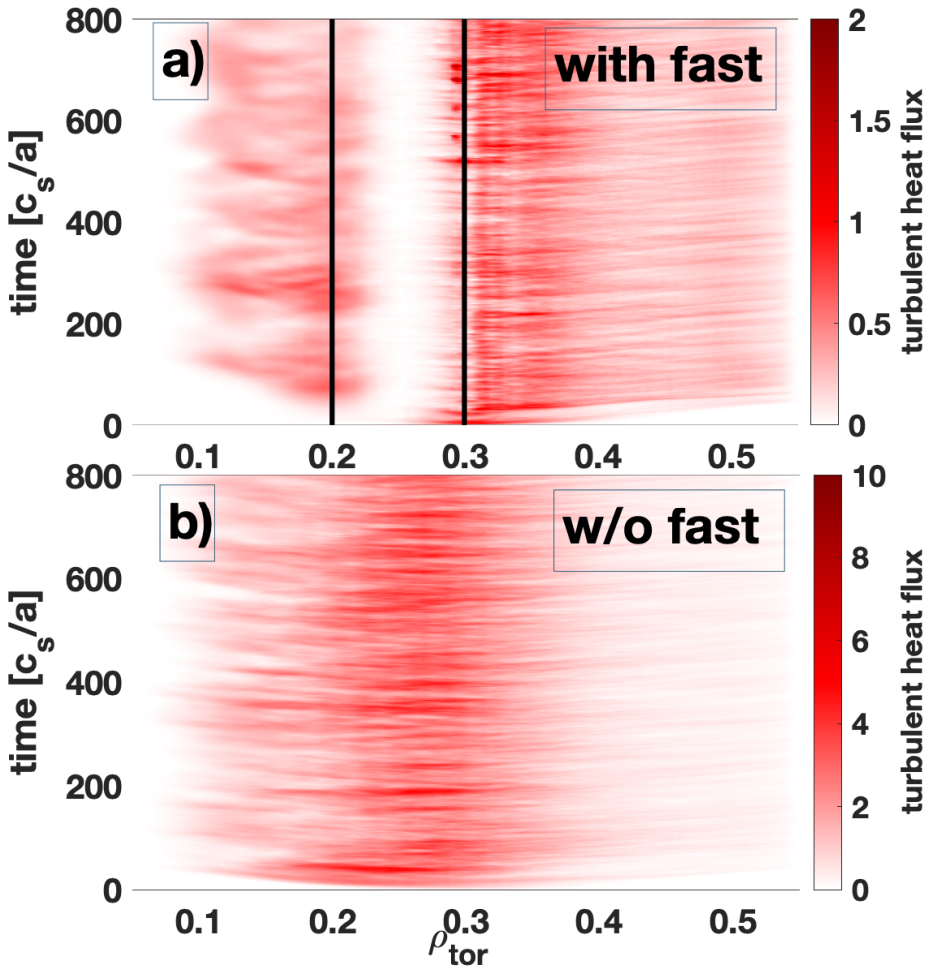

A. Di Siena et al. PRL 2021

Radial profile of $v_{E\times B_0}$

- Localised $E \times B_0$ shearing layers in the $v_{E\times B_0} = \partial_x \phi_1 / \rho_{tor} B_0$ observed at the radial boundaries of the transport barrier

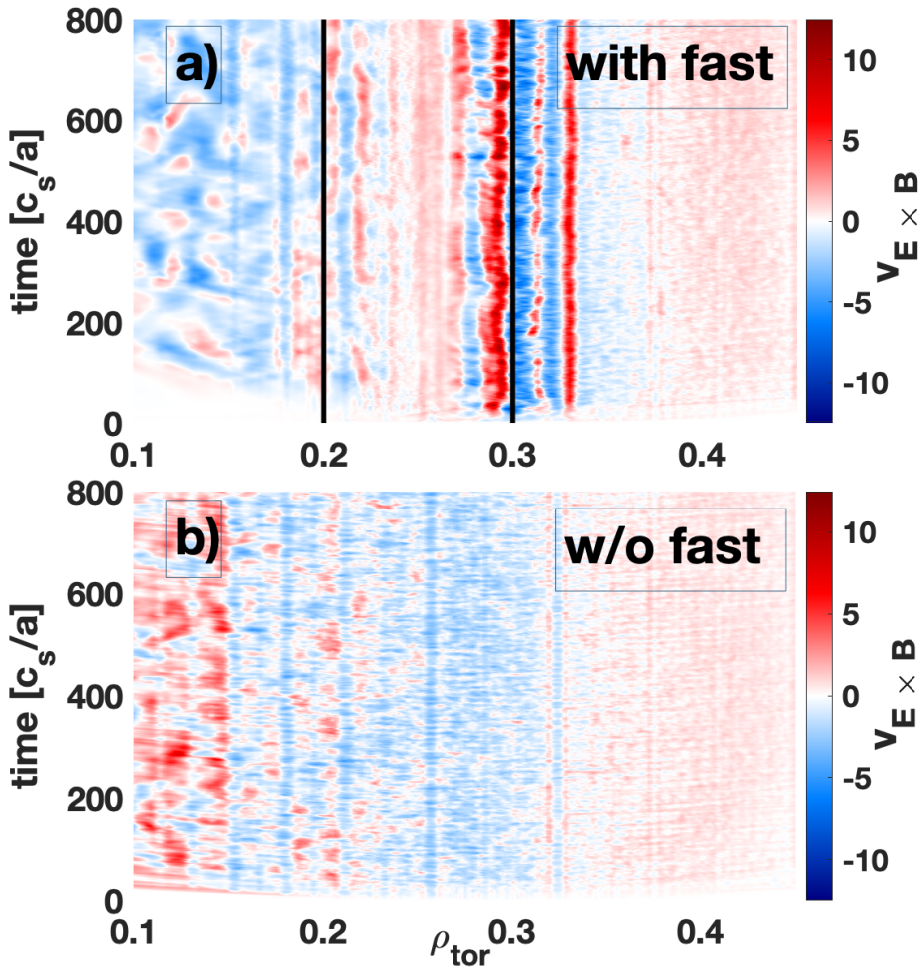

A. Di Siena et al. PRL 2021

Comparison with experimental power balance

- Excellent agreement between GENE and the volume integral of the injected sources computed by ASTRA.

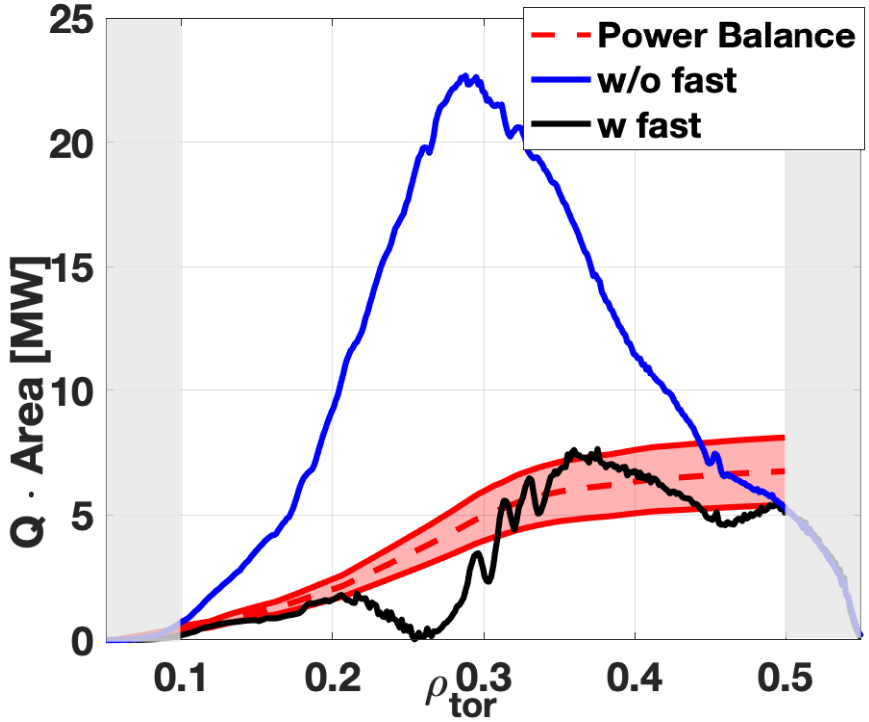

- GENE correctly reproduce experimental fluxes only when supra-thermal particles are retained.

A. Di Siena et al. PRL 2021

F-ATB in the SPARC H-mode scenario with 25 MW of ICRH heating

(Submitted to Nucl. Fusion)

SPARC H-mode scenario with 25 MW of ICRH power

- SPARC scenarios selected: $B_0 = 8.5$T; 25MW of ICRF power; 6.1MA plasma current → expected fusion gain $Q \sim 0.9$ as predicted by TRANSP/TGLF.
- Numerical setup: realistic geometry, ion-to-electron mass ratio, collisions, electromagnetic.
- Plasma profiles computed via TRANSP simulations: deuterium, tritium, electrons and hydrogen minority ($n_h/n_e = 5\,\%$).

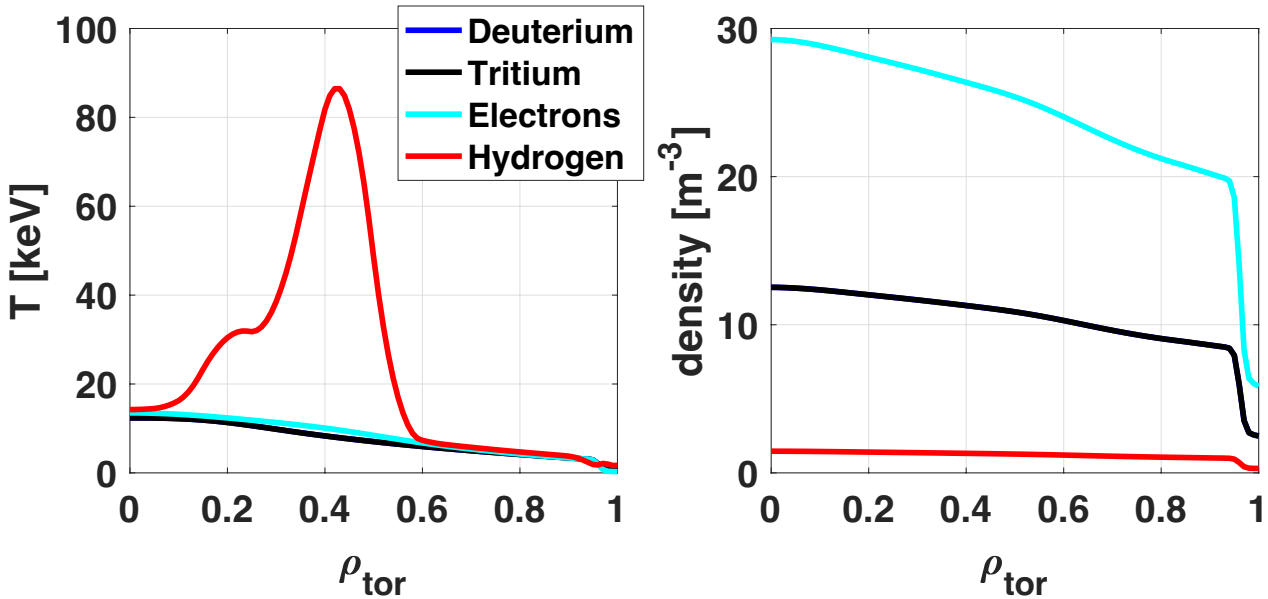

- Off-axis ICRH heating → optimal range of fast ion temperature and gradient between $\rho_{tor} \sim [0.44 - 0.6]$.

SPARC H-mode scenario with 25 MW of ICRH power

- SPARC scenarios selected: $B_0 = 8.5$T; 25MW of ICRF power; 6.1MA plasma current → expected fusion gain $Q \sim 0.9$ as predicted by TRANSP/TGLF.
- Numerical setup: realistic geometry, ion-to-electron mass ratio, collisions, electromagnetic.
- Plasma profiles computed via TRANSP simulations: deuterium, tritium, electrons and hydrogen minority ($n_h/n_e = 5\,\%$).

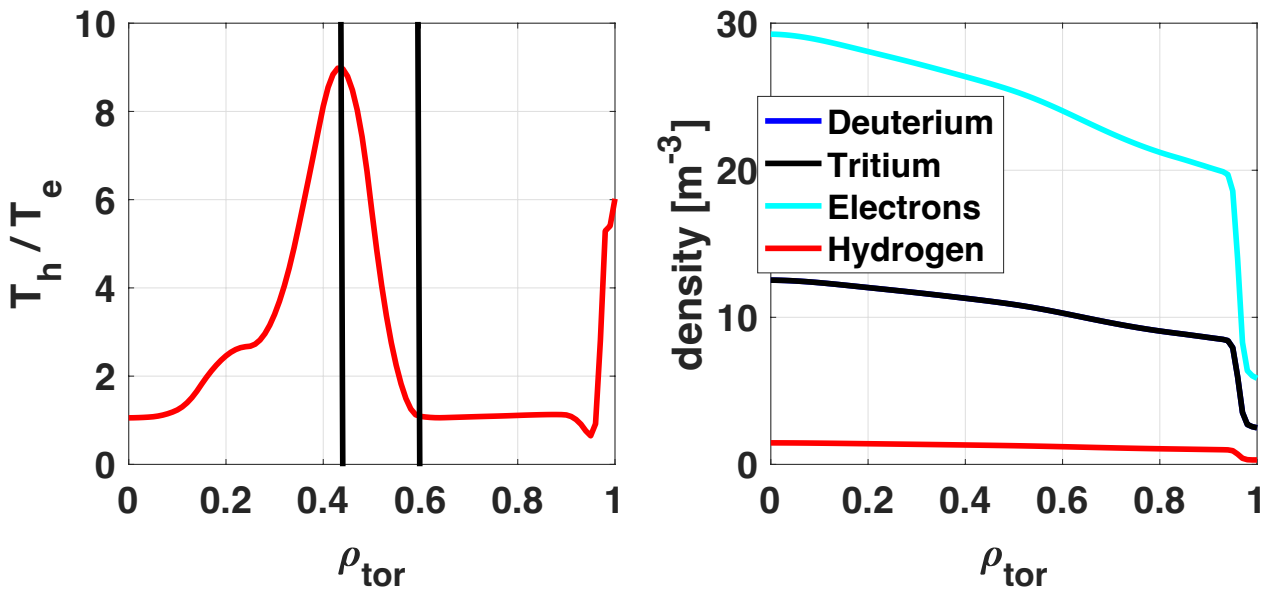

- Off-axis ICRH heating → optimal range of fast ion temperature and gradient between $\rho_{tor} \sim [0.44 - 0.6]$.

SPARC H-mode scenario - linear simulations at different locations

- Favorable fast ion parameters at $\rho_{tor} \sim 0.5 \rightarrow$ almost full linear stabilization observed.
- Enhanced stabilization expected at larger fast ion density (assuming similar T_f profiles) $\rightarrow$ ***room for optimization***

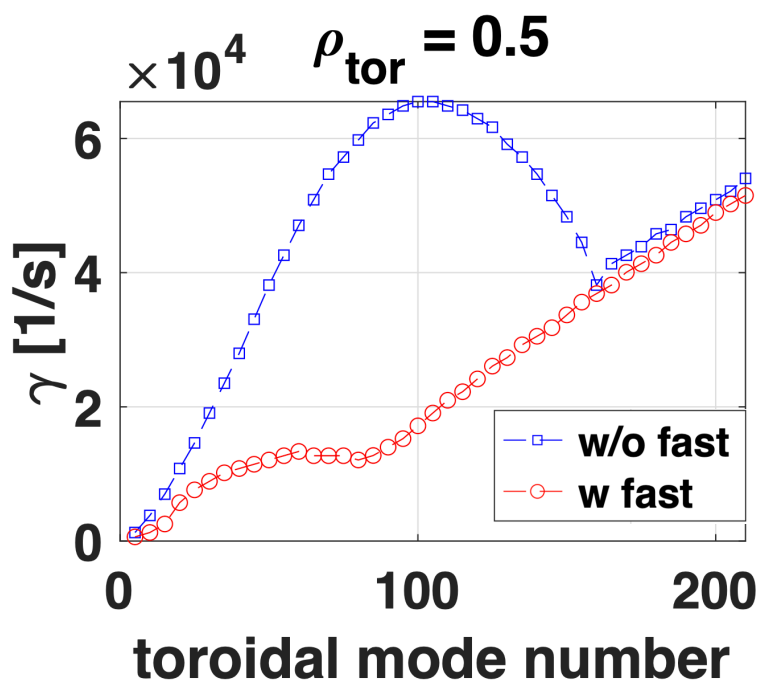

SPARC H-mode scenario - global nonlinear simulations: turbulent fluxes

- Transport barrier observed in the simulation retaining the ICRH fast particles: located in the region where the wave-particle resonant interaction is more effective $\rho_{tor} \sim [0.4 - 0.6]$

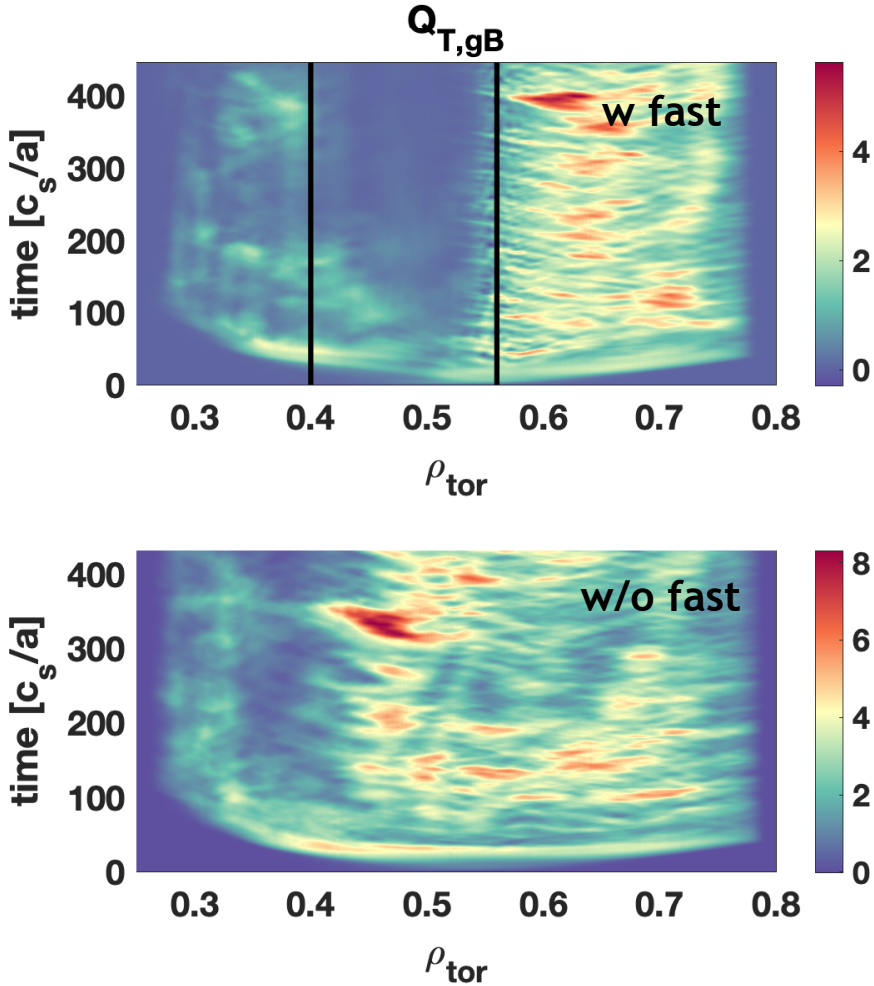

SPARC H-mode scenario - global nonlinear simulations: turbulent fluxes

- Transport barrier observed in the simulation retaining the ICRH fast particles: located in the region where the wave-particle resonant interaction is more effective $\rho_{tor} \sim [0.4 - 0.6]$

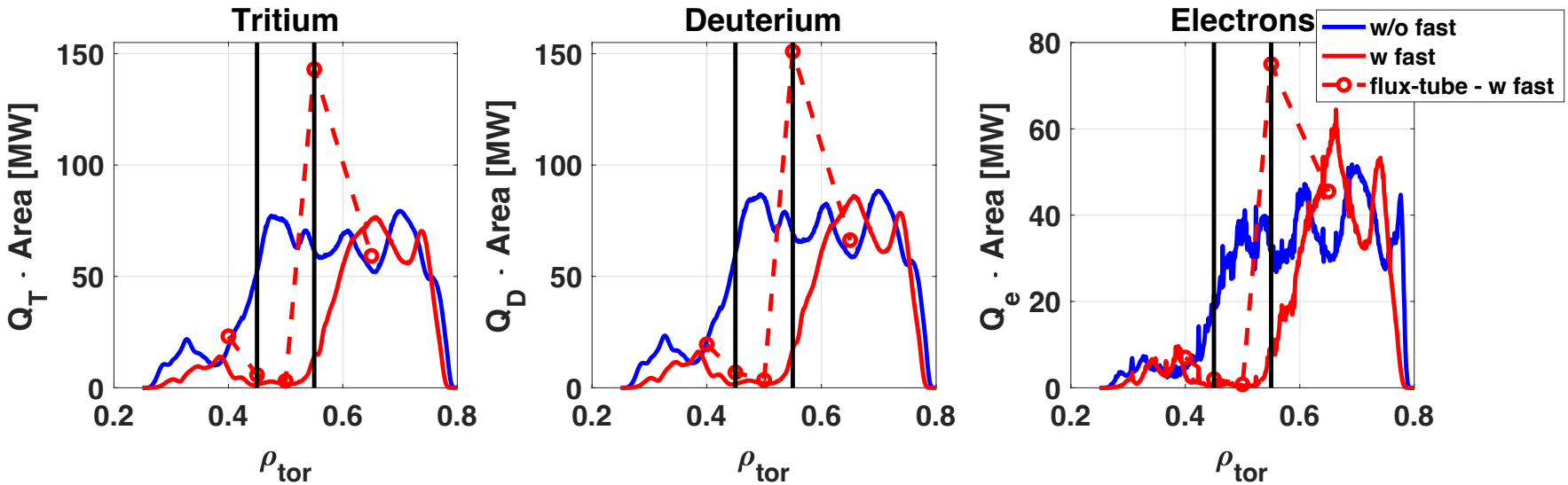

SPARC H-mode scenario - improved confinement

- More peaked ion temperatures could be observed → **fusion gain on this H-mode SPARC scenario might be underestimated by TRANSP/TGLF**

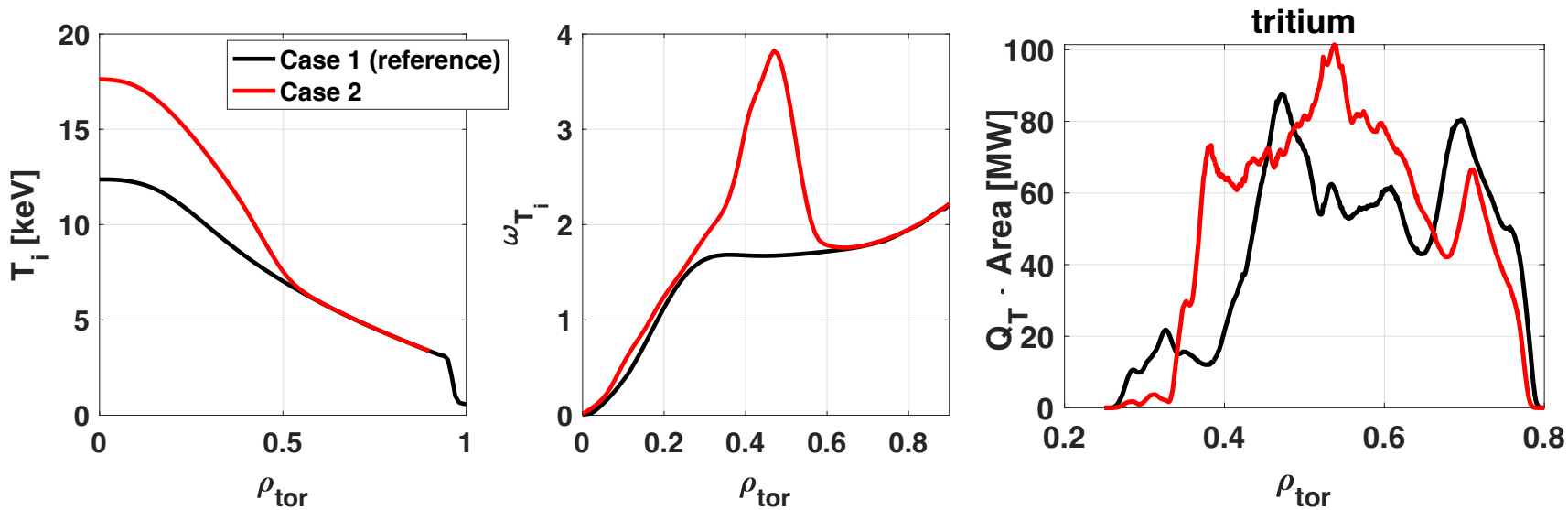

- Thermal ion profiles of Case 5 lead to an increase in fusion gain Q up to ~ 1.8.
- Onset of electromagnetic fast ion modes might limit the T_i-peaking → EM simulations with Case 5 are currently on-going.

$Q \sim 2$ might be achieved with off-axis heating!

Conclusions and on-going work

- Nonlinear electromagnetic stabilisation by energetic particles: marginally stable energetic particle modes excited nonlinearly → how accurate is the flux-tube description?

- Theoretical prediction and observation of a new type of transport barrier in gyrokinetic GENE simulations called F-ATB → can we exploit the wave-particle resonant mechanism at SPARC?

- Coupling the global version of GENE with transport code Tango to obtain steady-state profiles and study fast ion effects on turbulence *(see A. Di Siena NF 2022)*

- Impact of fusion-born alpha particles with GENE-Tango → beneficial/ detrimental to plasma confinement?